

A DCT-Based Broadband Multicarrier Transceiver

Shilpa Satish, Naofal Al-Dhahir and Hlaing Minn
Department of Electrical Engineering
University of Texas at Dallas, Richardson, TX 75083
aldhahir@utdallas.edu

Abstract

We investigate the use of the Discrete Cosine Transform (DCT) for multicarrier transmission over frequency selective channels. We derive design conditions for the DCT to diagonalize the channel into parallel, decoupled, and memoryless subchannels. Furthermore, we compare the performance of DCT and DFT-based multicarrier transceivers in the presence of channel estimation errors, residual frequency offset, and narrowband interference.

Keywords: Discrete Cosine Transform, Multi-Carrier Modulation, Guard Sequence, Frequency Selective Channel

1. Introduction

Multicarrier Modulation (MCM) based on the Discrete Fourier Transform (DFT) has been adopted as the modulation/demodulation scheme in several digital communications standards. These include wireline standards (such as ADSL) and wireless standards (such as DAB/DVB, IEEE 802.11a/g/n, and IEEE802.16a/e).

DFT-MCM divides the frequency response of the finite-impulse response (FIR) channel into parallel, decoupled, and memoryless subchannels using a guard sequence in the form of a cyclic prefix (CP). This CP is a periodic extension of the information symbols, converting the linear convolution of the FIR channel into circular convolution. Thus, the equivalent channel matrix can be perfectly diagonalized by the DFT, eliminating both inter-block interference (IBI) between symbols and inter-carrier interference (ICI) between adjacent frequency subchannels within each DFT-MCM symbol. Additional attractive features of using the DFT vectors as a modulation/demodulation basis include low computational complexity using the FFT algorithm and their independence of the channel characteristics.

In this paper, we show how to design a DCT-MCM transceiver that enjoys the above-mentioned desirable properties of DFT-MCM in addition to the following attractive features inherited from the DCT:

- The DCT basis is well-known to have excellent spectral compaction and energy concentration properties. Thus, in the presence of ICI it prevents excessive leakage into the adjacent subchannels [3].

- The DCT is widely adopted in image/video coding standards (e.g. JPEG, MPEG, H.261). Using it for modulation/demodulation on frequency selective channels results in a better integrated system design and a reduced overall implementation cost.
- The DCT uses real arithmetic compared to the complex-valued DFT. This reduces the computational complexity for the DCT-based processing and also reduces the signal power consumption.

However, we show that the main complexity disadvantage of DCT-MCM with respect to DFT-MCM is the need for a prefilter at the receiver to make the channel impulse response (CIR) symmetric in order for it to be diagonalizable by the DCT.

This paper is organized as follows. In Section II we describe the DCT-MCM transceiver model and derive its optimality conditions. Section III compares the performance of DFT-MCM and DCT-MCM under several practical impairments and the paper is concluded in Section IV.

2. DCT-MCM Transceiver

In this section we start by describing the mathematical model used for block transmission over a frequency selective channel. We show how the choice of the guard sequence affects the transceiver design. This is followed by a discussion on receiver signal processing including the key DCT-MCM channel diagonalization result.

2.1. Channel Model and Assumptions

We consider block by block transmission over a linear time-invariant (within the block) frequency selective noisy channel. The received symbols are given by

$$y_k = \sum_{m=-\nu}^{m=\nu} h_m x_{k-m} + z_k \quad (1)$$

where h_m is the m^{th} coefficient of the overall CIR which has memory of 2ν . The information symbols are assumed to be zero mean with an N-dimensional auto-correlation function R_{xx} . The additive white Gaussian noise (AWGN) symbols are denoted by $\{Z_k\}$ and have variance σ_z^2 . Additional 2ν guard symbols are added before

(v prefix symbols) and after (v suffix symbols) the information symbols to remove the IBI at the expense of a throughput loss factor of $\frac{2v}{N+2v}$. Furthermore, the $2v$ guard symbols are discarded at the receiver to eliminate their interfering effect. Equation (1) can be represented in matrix form as follows.

$$\begin{bmatrix} y_k \\ y_{k+1} \\ \vdots \\ y_{k+N-1} \end{bmatrix} = \begin{bmatrix} h_v & \cdots & h_0 & \cdots & h_{-v} & 0 & \cdots & 0 \\ 0 & h_v & \cdots & h_0 & \cdots & h_{-v} & 0 & \vdots \\ \vdots & \vdots & \ddots & \vdots & \ddots & \vdots & \vdots & 0 \\ 0 & \cdots & 0 & h_v & \cdots & h_0 & \cdots & h_{-v} \end{bmatrix} \begin{bmatrix} x_{k-v} \\ \vdots \\ x_{k-1} \\ x_k \\ \vdots \\ x_{k+N-1} \\ x_{k+N} \\ \vdots \\ x_{k+N+v-1} \end{bmatrix} + \begin{bmatrix} z_k \\ z_{k+1} \\ \vdots \\ z_{k+N-1} \end{bmatrix}$$

By partitioning the input vector into prefix, suffix and information symbols, we can write

$$\begin{aligned} y_{k:k+N-1} &= \mathbf{H}_{k-v:k+N+v-1} x_{k-v:k-1} + \mathbf{H}_{k:k+N-1} z_{k:k+N-1} \\ &= \mathbf{H}_{\text{pre}} x_{k-v:k-1} + \mathbf{H}_{\text{info}} x_{k-v:k-1} + \mathbf{H}_{\text{suf}} x_{k-v:k-1} + z_{k:k+N-1} \end{aligned} \quad (3)$$

Here, bold capital letters and small letters are used to denote matrices and vectors, respectively. Furthermore, the subscripts of the vector denote the indices of its first and last elements separated by a colon. The partitioning of the \mathbf{H} matrix is as follows

$$\begin{aligned} \mathbf{H}_{\text{pre}} &= \mathbf{H} \begin{bmatrix} \mathbf{I}_v \\ \mathbf{0}_{N \times v} \\ \mathbf{0}_{v \times v} \end{bmatrix}; \quad \mathbf{H}_{\text{suf}} = \mathbf{H} \begin{bmatrix} \mathbf{0}_{v \times v} \\ \mathbf{0}_{N \times v} \\ \mathbf{I}_v \end{bmatrix}; \\ \mathbf{H}_{\text{info}} &= \mathbf{H} \begin{bmatrix} \mathbf{0}_{v \times N} \\ \mathbf{I}_N \\ \mathbf{0}_{v \times N} \end{bmatrix}; \end{aligned} \quad (4)$$

Where \mathbf{I}_N denotes the identity matrix of size N and $\mathbf{0}_{N \times v}$ denotes the all-zero matrix with N rows and v columns. Refer [1] for more details. The two length- v guard sequences are redundant and they are related to the length- N information sequence by some deterministic functions as shown below.

$$x_{k-v:k-1} = \mathbf{G}_{\text{pre}} x_{k:k+N-1} \quad (5)$$

$$x_{k+N:k+N+v-1} = \mathbf{G}_{\text{suf}} x_{k:k+N-1}$$

Therefore, (3) can be written as

$$\begin{aligned} y_{k:k+N-1} &= (\mathbf{H}_{\text{info}} + \mathbf{H}_{\text{pre}} \mathbf{G}_{\text{pre}} + \mathbf{H}_{\text{suf}} \mathbf{G}_{\text{suf}}) x_{k:k+N-1} + z_{k:k+N-1} \\ &= \mathbf{H}_{\text{eqv}} x_{k:k+N-1} + z_{k:k+N-1} \end{aligned} \quad (6)$$

where \mathbf{H}_{eqv} is the $N \times N$ equivalent channel matrix. Equation (6) clearly shows the effect of different guard

sequence designs (through \mathbf{G}_{pre} and \mathbf{G}_{suf}) on the overall channel matrix \mathbf{H}_{eqv} . For example, for DFT-MCM, the guard sequences are chosen as cyclic extensions of the information sequence; i.e.

$\mathbf{G}_{\text{pre}} = \begin{bmatrix} \mathbf{0}_{v \times (N-v)} & \mathbf{I}_v \end{bmatrix}$ and $\mathbf{G}_{\text{suf}} = \begin{bmatrix} \mathbf{I}_v & \mathbf{0}_{v \times (N-v)} \end{bmatrix}$ We consider the type-II DCT defined by the real orthogonal matrix whose (l, m) entry is given by

$$C(l, m) = \begin{cases} \sqrt{\frac{2}{N}} \cos\left(\frac{(l-1)(2m-1)\pi}{2N}\right) & : 1 \leq l, m \leq N; l \neq 1 \\ \sqrt{\frac{1}{N}} & : l = 1 \end{cases}$$

here $\mathbf{C}^t \mathbf{C} = \mathbf{C} \mathbf{C}^t = \mathbf{I}_N$

Fact :

All $N \times N$ matrices diagonalizable by the type-II DCT matrix can be written as the sum of an $N \times N$ symmetric Toeplitz matrix \mathbf{T} and an $N \times N$ Hankel matrix \mathbf{L} , i.e. $\mathbf{C}(\mathbf{T} + \mathbf{L})\mathbf{C}^t = \mathbf{D}$, where \mathbf{D} is a diagonal matrix. Moreover, \mathbf{L} is determined from \mathbf{T} from the relations :

$$\begin{aligned} \mathbf{L}_1 &= \mathbf{S}_N \mathbf{T} \mathbf{e}_1 \\ \mathbf{L}_N &= \mathbf{J}_N \mathbf{L}_1 \end{aligned} \quad (7)$$

where \mathbf{S}_k is the $k \times k$ upper-shift matrix, \mathbf{J}_k is the $k \times k$ reversal matrix and \mathbf{e}_i is the i^{th} unit vector. For \mathbf{H}_{eqv} to be diagonalized by DCT it must satisfy the conditions in (7). Note that \mathbf{H}_{info} becomes a symmetric Toeplitz matrix if and only if

$$h_i = h_{-i} : 1, 2, \dots, v \quad (8)$$

which results in a symmetric linear-phase CIR. Next, we need to make the matrix $\mathbf{H}_{\text{pre}} \mathbf{G}_{\text{pre}} + \mathbf{H}_{\text{suf}} \mathbf{G}_{\text{suf}}$ a Hankel matrix that satisfies (7) in addition to (8). In order to satisfy the above constraint we choose

$$\begin{aligned} \mathbf{G}_{\text{pre}} &= \begin{bmatrix} \mathbf{J}_v & \mathbf{0}_{v \times (N-v)} \end{bmatrix} \\ \mathbf{G}_{\text{suf}} &= \begin{bmatrix} \mathbf{0}_{v \times (N-v)} & \mathbf{J}_v \end{bmatrix} \end{aligned} \quad (9)$$

The expressions for \mathbf{G}_{pre} and \mathbf{G}_{suf} in (9) imply that

$$x_{k-i} = x_{k+i-1} : 1 \leq i \leq v \quad (10)$$

$$x_{k+N+i-1} = x_{k+N-i} : 1 \leq i \leq v$$

This reveals that the guard sequences should be symmetric extensions of the information symbols.

2.2. Receiver Processing

The symmetry condition in (8) can be met in practice by implementing an FIR front-end prefilter, as follows:

- For channels with long memory, denoted by $L \geq (2\nu + 1)$, the design criterion used for the FIR channel shortening prefilter for DFT-based multicarrier is modified by incorporating the symmetry constraint on the target impulse response (TIR). In [4] it was shown that the channel shortening mean square error (MSE) can be expressed in the following quadratic form

$$MSE = \mathbf{h}' \mathbf{R} \mathbf{h} \quad (11)$$

where \mathbf{h} is the symmetric and shortened CIR and \mathbf{R} is a positive definite matrix that depends on the original CIR and the noise variance. The symmetric condition on \mathbf{h} in (8) can be imposed by defining

$$\mathbf{h} = \tilde{\mathbf{I}} \bar{\mathbf{h}} \quad (12)$$

Where $\bar{\mathbf{h}} = [h_0 \ \dots \ h_\nu]^t$ and $\tilde{\mathbf{I}} = \begin{bmatrix} \mathbf{I}_{\nu+1} \\ \mathbf{J}_\nu & \mathbf{0}_{\nu \times 1} \end{bmatrix}$.

Therefore, the channel shortening MSE becomes

$$MSE = \bar{\mathbf{h}}' \tilde{\mathbf{I}}' \mathbf{R} \tilde{\mathbf{I}} \bar{\mathbf{h}} = \bar{\mathbf{h}}' \bar{\mathbf{R}} \bar{\mathbf{h}} \quad (13)$$

subject to the constraint $\bar{\mathbf{h}}' \bar{\mathbf{h}} = 1$. The optimum $\bar{\mathbf{h}}$ is well known to be the eigenvector of $\bar{\mathbf{R}} = \tilde{\mathbf{I}}' \mathbf{R} \tilde{\mathbf{I}}$ corresponding to its minimum eigenvalue. The optimum symmetric shortened CIR is calculated using (12) and the optimum filter coefficients are determined from the Orthogonality Principle of Linear Estimation [5] using the Wiener equation (see [4] for details)

$$\mathbf{w} = \mathbf{R}_{yy}^{-1} \mathbf{R}_{yx} \mathbf{h} \quad (14)$$

where \mathbf{R}_{yx} and \mathbf{R}_{yy} are the output-input cross-correlation and the output auto-correlation matrices, respectively, which are calculated in closed form from the original channel matrix.

- For channels with short memory, we can still use the same prefilter but we need not shorten the channel. The length of the shortened channel is set equal to that of the CIR. In this case the CIR is just made symmetric without shortening it.
- For a short and real channel, the prefilter could be implemented as a matched filter. However this results in reduction of the channel throughput from $\frac{N}{N + \nu}$ to $\frac{N}{N + 2\nu}$.

2.3. Detection Algorithms

By properly designing the guard sequence and the prefilter, conditions (8) and (10) are satisfied. Starting from (6) we get

$$\begin{aligned} y_{k:k+N-1} &= \mathbf{H}_{\text{eqv}} \mathbf{x}_{k:k+N-1} + \mathbf{z}_{k:k+N-1} \\ &= \mathbf{C}' \mathbf{D} \mathbf{C} \mathbf{x}_{k:k+N-1} + \mathbf{z}_{k:k+N-1} \end{aligned} \quad (15)$$

$$\begin{aligned} \mathbf{Y}_{k:k+N-1} &= \mathbf{C} \mathbf{y}_{k:k+N-1} \\ &= \mathbf{D} \mathbf{X}_{k:k+N-1} + \mathbf{Z}_{k:k+N-1} \end{aligned}$$

where capital letters denote the DCT-transformed quantities. \mathbf{D} is a diagonal matrix whose elements are given by

$$d_i = \frac{\mathbf{e}_i' \mathbf{C} \mathbf{H}_{\text{eqv}} \mathbf{e}_1}{\mathbf{e}_i' \mathbf{C} \mathbf{e}_1} \quad (16)$$

The elements of $\mathbf{X}_{k:k+N-1}$ are thus decoupled and can be individually detected by applying a simple zero forcing (or MMSE) scalar equalizer followed by a slicer. See the DCT-MCM block diagram in Figure 1.

3. Comparison of DCT-MCM with DFT-MCM

In this section, we compare the performance of DCT-MCM with DFT-MCM in the presence of practical impairments such as channel estimation errors, residual frequency offset, and narrowband interference. We consider Channel B as specified in the wireless local area network (WLAN) ETSI HIPERLAN2 standard [6] which models a highly dispersive office environment with a large maximum delay spread of 730nec corresponding to a CIR with 16 symbol-spaced channel taps. We design a prefilter to shorten the CIR to a 5 tap impulse response for both DFT-MCM and DCT-MCM. For the latter, the prefilter makes the channel symmetric as well.

3.1. Frequency Offset

Multicarrier transceivers are more sensitive to frequency offset than single-carrier transceivers since in the former, information is transmitted over narrowband orthogonal subcarriers. Any residual frequency offset will cause ICI which degrades performance. The frequency offset model is implemented as a diagonal matrix where each entry specifies the offset at that time instant. The frequency offset effect is modeled using the diagonal matrix

$$\mathbf{S} = \text{diag} \left(e^{\frac{j2\pi f_o i}{N}} \right) : 0 \leq i \leq N + 2\nu - 1 \quad (17)$$

where f_o is the normalized (by subchannel width) frequency offset. The equivalent channel matrix is then given by

$$\mathbf{H} = \mathbf{W} * \mathbf{S} * \mathbf{H}_{\text{orig}} \quad (18)$$

where \mathbf{W} is the prefilter convolution matrix and \mathbf{H}_{orig} is the original channel convolution matrix. All matrices are of

size $(N + 2\nu) \times (N + 2\nu)$. The guard sequence of size 2ν is stripped at the receiver.

The performance of DFT-MCM and DCT-MCM is compared in Fig. 2 for block size $N=64$ using the achievable bit rate criterion averaged over 10000 channel realizations for normalized frequency offsets ranging from 0.01 and 0.1 and input SNR of 20dB. The number of prefilter coefficients used is 64. The bit rate is calculated using the ‘‘gap approximation’’ [2] at a target error rate of 10^{-6} assuming a coding gain of 4.5 dB. The figure shows that DCT-MCM outperforms DFT-MCM with increasing frequency offset. An increase in frequency offset increases the ICI. Since the DCT has better spectral containment properties than the DFT, the ICI leakage into adjacent subcarriers is less compared to DFT and hence it achieves better performance which also corroborates the results in [3].

3.2. Channel Estimation with Frequency Offset

The channel is estimated in the presence of frequency offset using training symbols. The received symbol at time k is modeled as

$$y(k) = e^{j2\pi f_o k} \sum_{i=0}^{2\nu} h(i)x(k-i) + z(k) \quad (19)$$

where $\{x(m)\}$ is the training sequence and $e^{j2\pi f_o k}$ is the frequency offset at time instant k . Writing (19) in matrix form, we get

$$\mathbf{y} = \mathbf{S}\mathbf{X}\mathbf{h} + \mathbf{Z} \quad (20)$$

where \mathbf{X} is a Toeplitz matrix of size $(N_t - 2\nu + 2) \times 1$ composed of root-of-unity training symbols[7], \mathbf{h} is the CIR vector of size $2\nu + 1$ and N_t is the length of the training sequence. Without correction of the residual frequency offset, the least-squares channel estimate is given by

$$\mathbf{h}_{est} = (\mathbf{X}'\mathbf{X})^{-1} \mathbf{X}'\mathbf{y} \quad (21)$$

where $(\cdot)'$ denotes the complex-conjugate transpose. As in (18), the equivalent channel is calculated as

$$\mathbf{H} = \mathbf{W} * \mathbf{S} * \mathbf{H}_{est} \quad (22)$$

The performance of DFT-MCM and DCT-MCM is compared for $N=64$ using the bit rate criterion averaged over 10000 channel realizations for normalized frequency offsets ranging from 0.01 and 0.1 and input SNR of 20dB. The length of the training sequence was taken to be 64 and the number of prefilter coefficients is 64. The channel was assumed constant over 4 consecutive blocks over which the estimate was averaged to reduce noise effects.

Fig. 3 shows that DCT-MCM still outperforms DFT-MCM with increasing offset. However, the cross-over

point shifted to higher frequency offsets because of the increased sensitivity of DCT-MCM compared to DFT-MCM to channel estimation errors. This can be attributed to the additional requirement of an overall symmetric CIR for DCT-MCM which increases the sensitivity to channel estimation errors.

3.3. Narrowband Interference (NBI)

The scarcity of radio frequency spectrum necessitates spectral coexistence of several wireless systems with different transmission bandwidths. One consequence of this spectral overlap is narrowband interference to multicarrier systems which can affect several subchannels causing performance loss. In this paper, NBI is modeled as Gaussian correlated noise [8] with auto correlation

$$\text{sequence } R_{ii}(k) = \left(\frac{\sin(\omega_a k / 2)}{\omega_a k / 2} \right) \cos(\delta\omega k) \quad (23)$$

where ω_a is the bandwidth of the interferer and $\delta\omega$ is its center frequency (in radians). If J_o is the total jammer power, then the jammer power per affected subchannel is given by

$$J = \frac{J_o * N_{spread}}{N} \quad (24)$$

where N_{spread} is the number of subcarriers over which the interference is spread. If f_{cNBI} is the center frequency of the interference in Hz, then

$$\delta\omega = \frac{2 * \pi * f_{cNBI}}{BW} \quad (25)$$

where BW is the total bandwidth of the channel in Hz. Knowing J_o , $\delta\omega$, and ω_a , the symmetric Toeplitz interference auto-correlation matrix can be calculated using (23). Then, the overall noise autocorrelation matrix is given by

$$R_{nn} = J_o * R_{ii} + \sigma_z^2 \mathbf{I} \quad (27)$$

Here, σ_z^2 is the variance of the white Gaussian noise floor. The performance of DFT-MCM and DCT-MCM is compared for $N=64$ for different jammer to noise power ratios (JNR) at input SNR=20 dB using the bit rate criterion averaged over 10000 realizations.

The bandwidth of the channel was taken to be 20MHz and the center frequency of the jammer was assumed to be 3MHz. In one case, the interference was assumed to affect only two subchannels and in the second case, it affected 4 subchannels. JNR was varied from -10dB to 60 dB. The number of prefilter coefficients was 64.

Fig. 4 shows that for moderate to high JNR, DCT-MCM outperforms DFT-MCM. Also, as the number of

subchannels affected by NBI increases, the reduction in bit rate is more graceful for DCT-MCM. This demonstrates the improved robustness of DCT-MCM compared to DFT-MCM in the presence of NBI due to the superior spectral compaction and energy concentration properties of the DCT which reduce excess leakage of the ICI energy into adjacent subchannels and hence result in better performance.

4. Conclusion

The DCT is an optimal modulation/demodulation basis when the overall CIR is symmetric and the prefix and suffix guard sequences are a symmetric extensions of the information symbols in each transmitted block. The first condition can be met by implementing an FIR prefilter and the second condition can be met by placing symmetry conditions only on the guard sequence.

DCT-MCM has comparable complexity to DFT-MCM for long channels where both transceivers require a prefilter to limit the guard sequence throughput overhead. However, for short channels, DCT-MCM still requires a prefilter (unlike DFT-MCM) which can be implemented as a time reversed matched filter. Both DFT-MCM and DCT-MCM can perfectly diagonalize frequency selective channels without channel knowledge at the transmitter.

Our simulations show that DCT-MCM is more robust to frequency offset and narrowband interference than DFT-MCM. Both impairments result in intercarrier interference which leaks into adjacent subcarriers. However, the enhanced spectral containment property of the DCT (compared to DFT) results in better performance.

In summary, our results in this paper show that DCT-MCM is a viable multicarrier transceiver which can be competitive with DFT-MCM in some practical scenarios. Our ongoing research includes comparison of DFT-MCM and DCT-MCM in a wireless environment in the presence of I/Q imbalance, timing offset, and Doppler (mobility) conditions. In addition, we are comparing the performance of both transceivers in a realistic ADSL environment.

5. Acknowledgements

The work of N. Al-Dhahir is supported in part by ATP contract 009741-0023-2003 and by NSF contracts CCF 0430654 and DMS 0528010.

6. References

[1] N. Al-Dhahir, H. Minn, S. Satish, "Optimum DCT-Based Multicarrier Transceivers for Frequency-Selective Channels". To appear in IEEE Transactions on Communications, 2006.
 [2] J. Cioffi, "A Multicarrier Primer". In ANSI T1E1.4 Committee contribution no. 91-157. Available online <http://www.stanford.edu/group/cioffi/pdf/multicarrier.pdf>

[3] P. Tan and N. Beaulieu, "Precise Bit Error Rate Analysis of DCT OFDM in the presence of Carrier Frequency Offset on AWGN Channels". In IEEE Globecom Conference, November 2005.
 [4] N. Al-Dhahir and J.M.Cioffi. "Efficiently-Computed Reduced-Parameter Input-Aided MMSE Equalizers for ML Detection: A Unified Approach". IEEE Trans. Information Theory, Page(s):903-915, May 1996
 [5] T. Kailath, A. Sayed and B. Hassibi. Linear Estimation. Prentice Hall, 2000.
 [6] ETSI Normalization Committee. Channels for HIPERLAN/2 in Different Indoor Scenarios. Document No. 3ER1085B. Sophia-Antipolis, France, 1998.
 [7] C. Fragouli, N. Al-Dhahir and W. Turin. "Training-Based Channel Estimation for Multiple-Antenna Broadband Wireless Communications", IEEE Transactions, Page(s):384 – 391, March 2003.
 [8] L. B. Milstein and R. A. Iltis. "Signal Processing for Interference Rejection in Spread Spectrum Communications". IEEE ASSP Magazine, Page(s):18 – 31, April 1986.

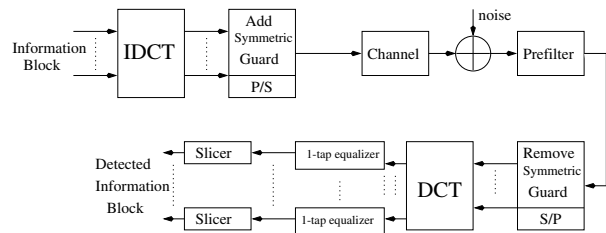


Figure 1. DCT-MCM block diagram for baseband signaling

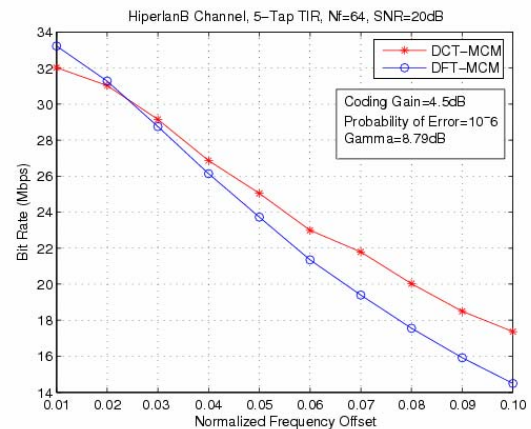


Fig 2. Achievable bit rates at different frequency offsets

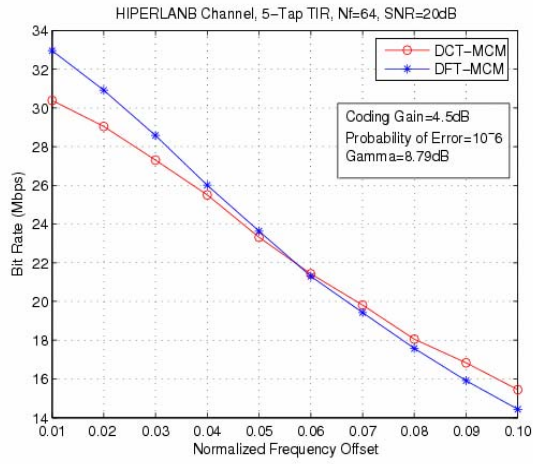


Fig 3. Achievable bit rates with estimated channel at different frequency offsets

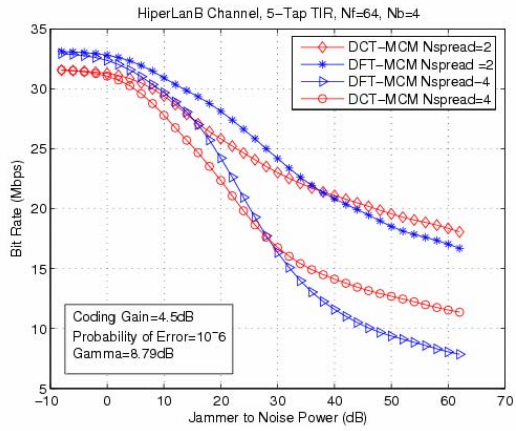


Fig 4. Achievable bit rates at different jammer to noise power ratios